J. ADV. SIMULAT. SCI. ENG.
Vol. 6, No. 1, 273-281.

MMLPA: Multilayered Metamaterial Low Profile Antenna for IoT Applications

Tojoarisoa Rakotoaritina[1,*], Megumi Saito[1], Zhenni Pan[1], Jiang Liu[1], Shigeru Shimamoto[1]

[1]Department of Computer Science and Communications Engineering, Waseda University

[*]tojoarisoa@toki.waseda.jp

Received: November 22, 2018; Accepted: July 21, 2019; Published: August 10, 2019

Abstract. Nowadays, within the concept of Internet of Things (IoT), smart homes, smart factory, intelligent transportation among others are infrastructure systems that connect our world to the Internet. However, wireless communications technology are considerably constrained by complicated structures, and lossy media in complex environments. Fundamental limitations on the transmission range have been treated to connect IoT devices in such Radio Frequency (RF) challenging environments. In order to extend the transmission range in complex environments, Magnetic Induction (MI) communication has been proved to be an efficient solution. In this paper, a Multilayered Metamaterial low profile antenna (MMLPA) using Magnetic Induction communication scheme is proposed for IoT applications. The system model of the MMLPA is analyzed. Then an MMLPA system is designed by using a circular loop antenna backed with isotropic metamaterial which is considered as a Defected Ground Structure (DGS) as well as with anisotropic metamaterial for the purpose of a dielectric uniaxial metamaterial. By using a full-wave finite-element method, the proposed analysis is supported with simulation results where good agreement is achieved compared to the measurement results after realizing four prototypes of the MMLPA antennas. The effect of the presence of metal in the vicinity of the transceivers is also analyzed.

Keywords: IoT, low profile antenna, metamaterial antenna, Magnetic Induction, MMLPA, near metal environment.

1. Introduction

In this paper, Multilayered Metamaterial Low Profile Antennas (MMLPA) using Magnetic Induction communication scheme are designed and prototyped for IoT applications. To the best of our knowledge, this is the first work that investigates the performance of a magnetic loop antenna coil backed with multiple layers of isotropic and anisotropic metamaterials for IoT applications in environment that are hostile, RF challenged, and especially in the vicinity of metal. The proposed analysis is supported with simulation results by using a full-wave

finite-element method, where good agreement is achieved compared to the measurement results after realizing four prototypes of the MMLPA antennas.

2. MMLPA-IoT Application overview

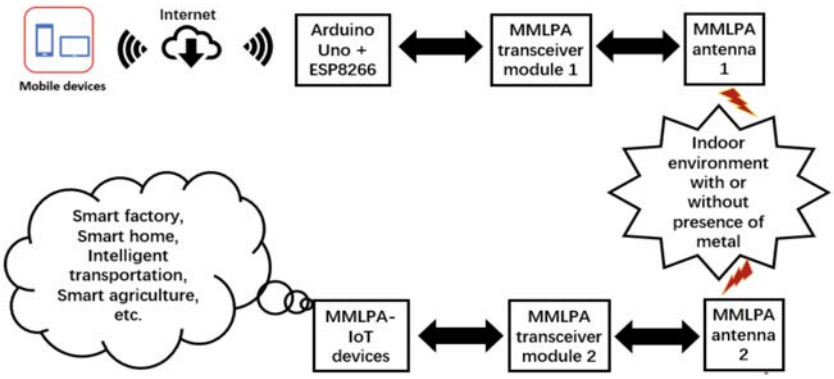

Figure 1: MMLPA-IoT application system setup.

The objective of this work is to design and realize the proposed system shown in Fig. 1 by using MMLPA antennas. In this system, orders can be send from smartphone or tablet to remotely control MMLPA-IoT devices via Internet. This action can be done automatically or scheduled according to the desired applications. MMLPA-IoT is defined here as a network of MMLPA-IoT devices embedded with sensors, MMLPA antenna modules and network connectivity, so that they can collect, exchange, and act on data with or without human intervention and even in complex environments. There are various applications for this system including smart industry, smart home, intelligent transportation, smart agriculture, etc.

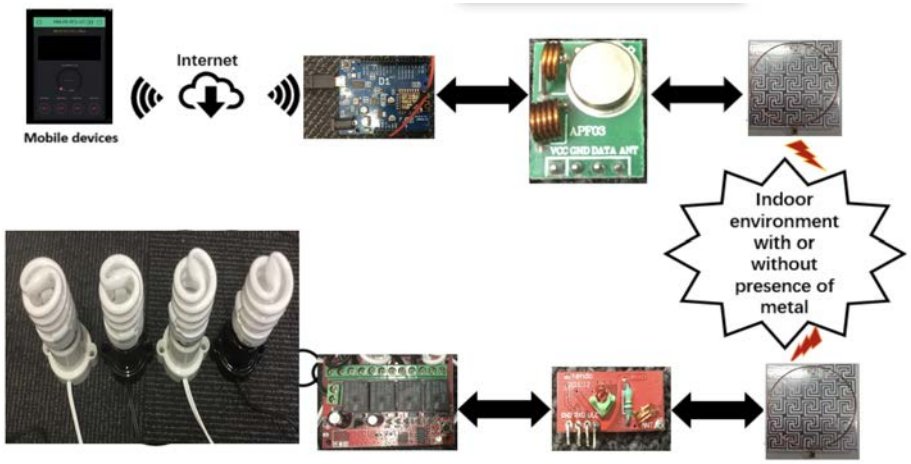

Figure 2: MMLPA-RCS-IoT system.

The application for home automation has been performed by using this system as a Remote Control Switch (RCS), which is to remotely control power outlet sockets, lamps and some home appliances. For example, an MMLPA-RCS-IoT application was developed and installed on iPad, as shown in Fig. 2, which aims to control four electrical switches remotely using Internet connection.

3. System model

According to previous work in [1], an equivalent circuit can be modelled, as shown in Fig. 3, for the channel of the MMLPA communication system.

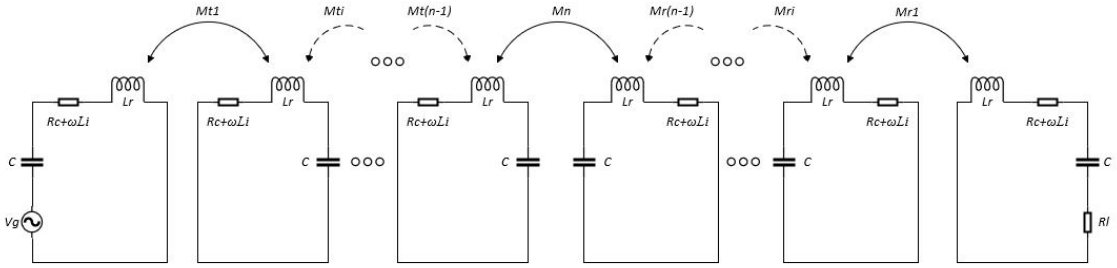

Figure 3: Equivalent circuit model of MMLPA communication.

Where: *Vg* is the source voltage; *Rc* is the resistance of the coil; *Lr* is the self-inductance of the coil; *C* is the compensation capacitor which is used to tune the circuit at resonant; *Mn* is the mutual inductance between MMLPA transmitter and MMLPA receiver. *Mt1,..., Mt(n-1)* are the mutual inductance between the transmitter loop antenna coil and the first layer of metamaterials composed with isotropic and anisotropic metamaterials at the transmitter side, ..., the mutual inductance between the *(n-1)-th* and the *n-th* layers of metamaterials at the transmitter side respectively. Similarly, *Mr1,..., Mr(n-1)* are the mutual inductance between the receiver loop antenna coil and the first layer of metamaterials at the receiver side, ..., the mutual inductance between the *(n-1)-th* and the *n-th* layers of metamaterials at the receiver side respectively; *Rl* is the load resistance.

In MMLPA system, as illustrated in Fig. 4, the performance of MI communication using loop antenna coil can be enhanced when it is backed with *n* layers of metamaterials. The number of metamaterial layers can be set as well as its thickness while keeping the size of the antenna small and making it low profile.

Based on the equivalent circuit represented in Fig. 3, the path loss for MMLPA channel, which is the main factor that decides the transmission range, is derived:

$$PL \approx -20(2n-1)\log(\frac{\omega|M|}{Rc+\omega Li}) \tag{1}$$

where: n is the number of metamaterial layers, ω is the angular frequency, Li is the imaginary part of the self-inductance, and it is assumed that all the mutual inductances are equal to M.

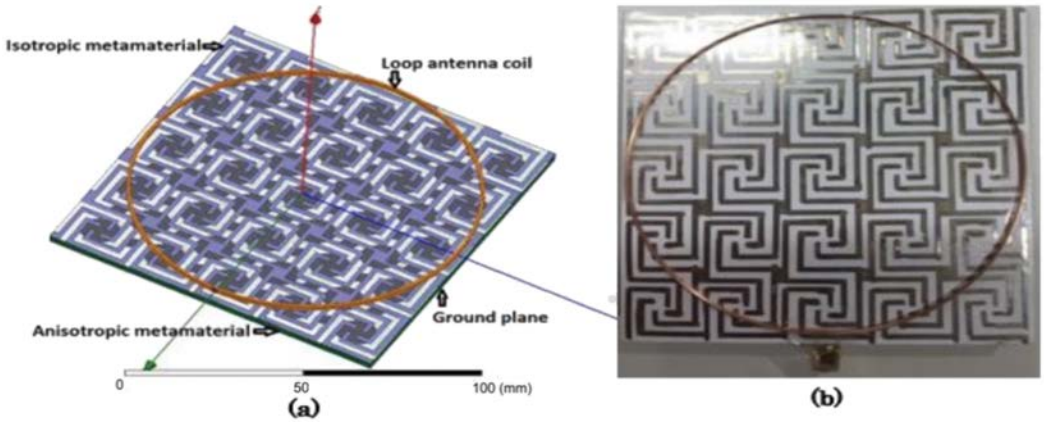

Figure 4: MMLPA system: (a) the designed antenna, (b) the prototyped antenna.

In this work, air is considered as the transmission medium with presence or absence of metal in the vicinity of the MMLPA transceivers. Therefore, according to the Friis transmission equation, the communication range d_{tr} is derived as below.

$$d_{tr} = \frac{c\sqrt{GtGr}}{2\pi\omega}\left(\frac{Rc + \omega Li}{\omega|M|}\right)^{2n-1} \tag{2}$$

where: c is the velocity of light, Gt and Gr are the gain of the transmitting and receiving antennas respectively.

A normally incident plane wave on a metamaterial placed in free space is represented in Fig. 5 below.

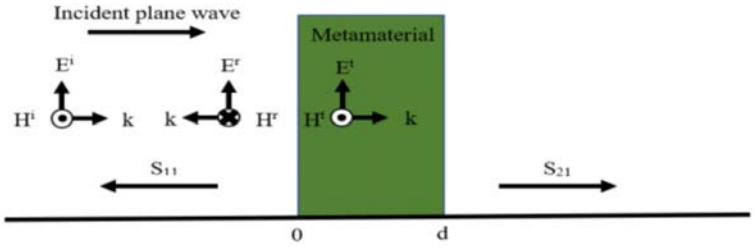

Figure 5: A normally incident plane wave on a metamaterial placed in free space.

According to [2], the return loss of this system can be derived as:

$$S_{11} = \frac{R_{01}(1 - e^{i2refk_0d})}{1 - {R_{01}}^2 e^{i2refk_0d}} \tag{3}$$

where:

$$R_{01} = \frac{z-1}{z+1} \tag{4}$$

z is the impedance, ref is the refractive index, k_0 is the wave number, d is the maximum length of the unit element of the metamaterial.

The coil antenna is made by copper wire with: inner diameter 100 mm, outer diameter 101.6 mm, thickness 2.13 mm and 52 turns. In this work, we consider two layers of metamaterial. The four-arm spiral geometry shown in Fig. 6 has been proven to successfully eliminate the cross polarized fields [3]. Therefore, this shape is designed here as the first layer of the isotropic metamaterial to back the loop antenna coil since it can also enhance the magnetic field intensity for a directional field distribution. Its unit element is designed by using circuit marker pen with a silver ink on a photo paper 105 mm x 105 mm. Therefore, the conductive area is drawn in black as shown in Fig. 6 below.

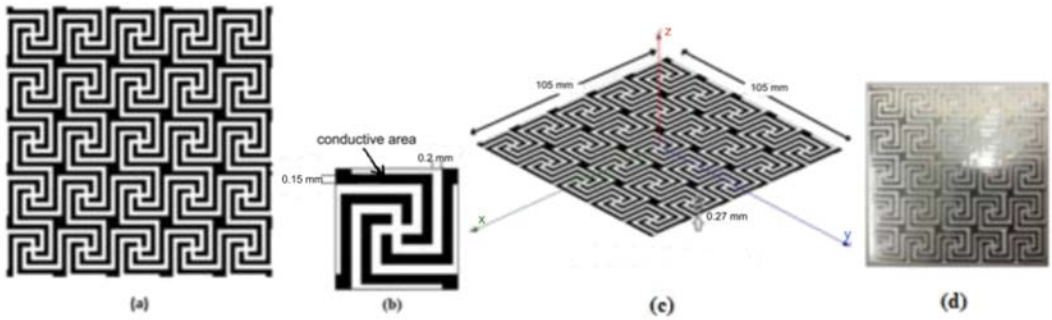

Figure 6: Proposed isotropic metamaterial: (a)unit element (UE), (b)unit cell (UC), (c)designed UE, (d)prototyped UE.

The second layer is an anisotropic metamaterial which is utilized to be the polarization tunable absorber. The number of metamaterial layers can determine the frequency for the maximum absorption and it can also increase the bandwidth. Therefore, it is better to increase the thickness of the metamaterial layers at the receiver side. In this work, two types of anisotropic metamaterial are manufactured by 3D printing as shown in Fig. 7 by considering the methodology shown in [4] of a uniaxial metamaterial in order to improve the working efficiency of the MMLPA antenna.

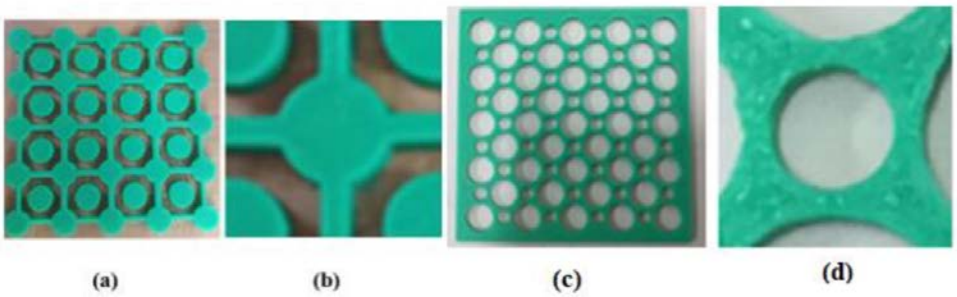

Figure 7: Two types of anisotropic metamaterials: (a) unit element 1, (b) unit cell 1, (c) unit element 2, (d) unit cell 2.

4. Simulation and experimental results

Four prototypes of the system have been realized and measured as shown in Fig. 8 below.

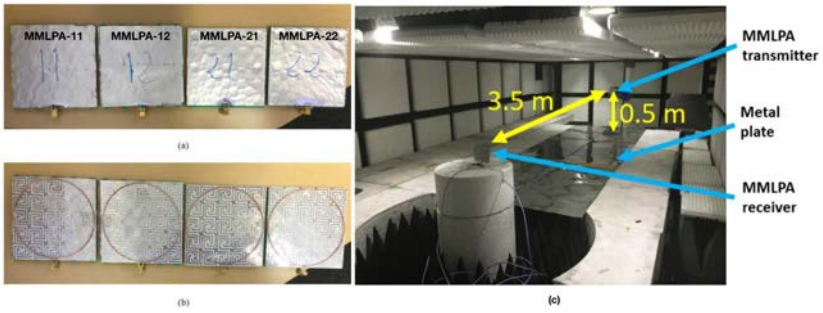

Figure 8: (a)/(b):proposed MMLPA prototypes (front view (a) and back view (b)), (c):experiment setup inside an anechoic chamber.

Where: MMLPA-11 is a circular loop antenna backed with anisotropic metamaterial type 1 and its thickness is t_{am1} = 3 mm; MMLPA-21 is a circular loop antenna backed with anisotropic metamaterial type 2 with the same thickness t_{am1} ; MMLPA-12 is a circular loop antenna backed with anisotropic metamaterial type 1 and its thickness is t_{am2} = 5 mm; MMLPA-22 is backed with anisotropic metamaterial type 2 with the same thickness t_{am2}. It is important to note that each of these antennas has the same specifications and geometries for the loop antenna coil, the isotropic metamaterial and the ground plane.

According to [5], the requirements of wireless IoT are low power, low cost, medium range, and moderate data rate. Consequently, it is reasonable to assume that the operating frequency should be between 100 MHz and 5.8 GHz, since lower frequencies would not allow for sufficient data rate while higher frequencies would have very short range. In this paper, 315 MHz and 2.4 GHz are chosen as frequencies of operation of our MMLPA-IoT system, since they belong to the unlicensed bands in this range between 100 MHz and 5.8 GHz, they are utilized almost worldwide as well.

The following figures are the simulation results for the MMLPA-11 at 2.4 GHz using HFSS software. The return loss is shown in Fig. 9 and it is compared with the measurement result.

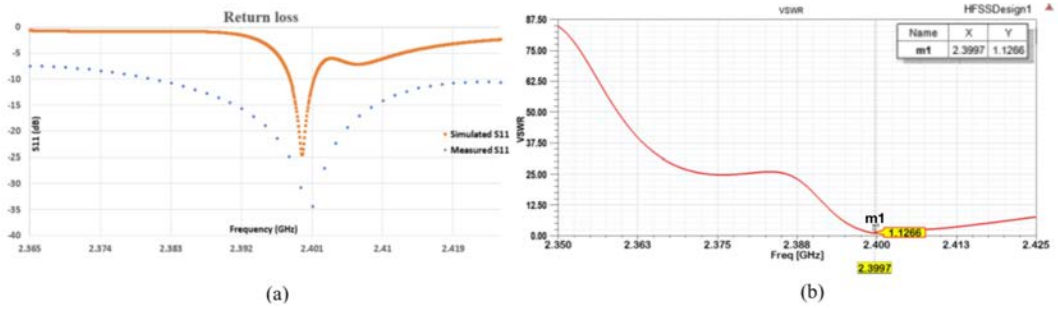

Figure 9: MMLPA-11. (a)Return loss at 2.4 GHz, (b)VSWR at 2.4 GHz.

The scattering parameter S_{11} acts as return loss since the antenna is a one-port device. The simulated return loss of MMLPA-11 is shown in Fig. 9, it is equal to -24.5052 dB at resonant frequency 2.3997 GHz while it is equal to -34.26 dB after measurement. The slight difference is due to the assumption taken during the simulation which is related to the mutual inductance as discussed above and the cable loss during the measurement. A VSWR of 1.12 has less than 4% of reflected power. In other words, more than 96% of the power is delivered to the antenna.

In addition, a graphical presentation of signal distribution of the antenna is given by radiation pattern. The two-dimensional (2D) and three-dimensional (3D) radiation patterns for MMLPA-11 at 2.4 GHz are obtained as shown in Fig. 10(a) and Fig. 10(b) respectively.

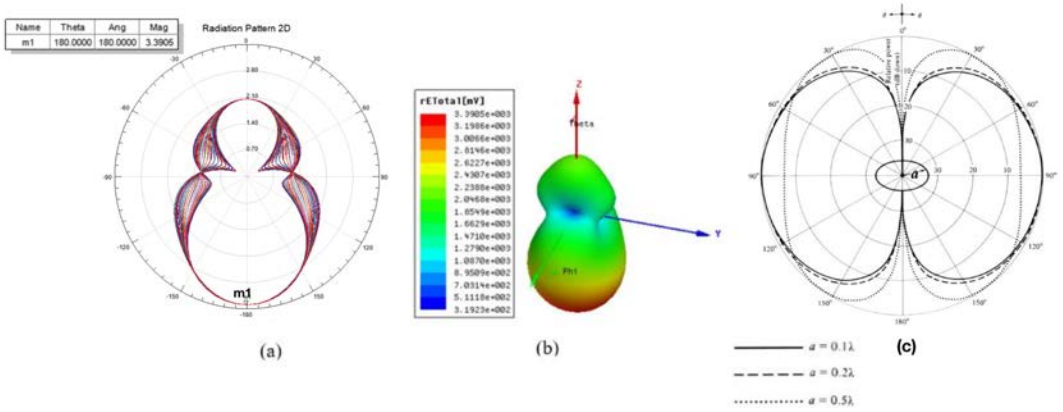

Figure 10: MMLPA-11. (a) Radiation pattern 2D, (b) Radiation pattern 3D, (c) Radiation pattern for a circular loop antenna without the metamaterial layers.

By comparing Fig. 10(a) to Fig. 10(c) [6], the field radiated along the axis of a circular loop antenna without the metamaterial layers is zero. However, the field radiated by the MMLPA-11 along xy plane which is perpendicular to the axis of the circular loop antenna coil is zero. In other words, the metamaterial layers enhance the magnetic field intensity in one directional field distribution as shown in Fig. 11(c). The two- and three-dimensional directivity patterns of MMLPA-11 at 2.4 GHz are also represented in the Fig. 11(a) and Fig. 11(b) respectively.

In the experiment setup shown in Fig. 8, MMLPA-11 and MMLPA-21 are utilized as transmitters while MMLPA-12 and MMLPA-22 are the receivers, respectively. 315 MHz is chosen as operating frequency and the transmitted power is 10 dBm. The communication range is set at 3.5 m and the experiment is performed inside an anechoic chamber. In this work, a metal plate 1 m x 3 m made by steel is placed in between the transmitter antenna (Tx) and the receiver antenna (Rx). The height is 0.5 m from the surface of the metal plate to the axis of the antennas. For the first scenario, an additional power of 4.22 dBm is received at the receiver MMLPA-12 with the metal plate compared to the received power without the metal plate. For the second scenario, an additional power of 6.68 dBm is received at the receiver MMLPA-22 with the metal plate compared to the received power without the metal plate. By comparing the results of both scenarios, an additional power of 10.77 dBm

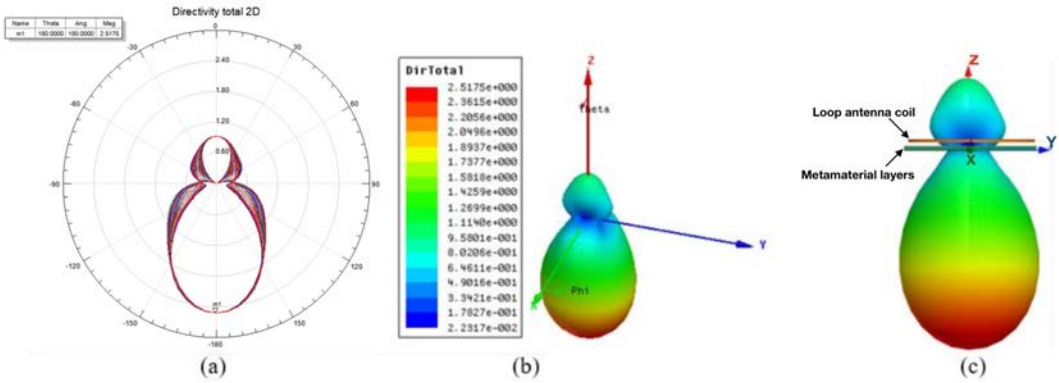

Figure 11: MMLPA-11. (a) Directivity total 2D, (b) Directivity total 3D, (c) Directivity total 3D in profile view with the antenna.

is received at the receiver when using the antennas backed with anisotropic metamaterials type 1. Therefore, the type 1 has stronger directivity than the type 2 and the presence of metal in the vicinity of MMLPA transceivers increases the received power. As a result, the communication range is also increased.

5. Conclusion

It has been shown that good agreement is achieved between simulation and measurement results of our MMLPA antenna. Its magnetic field intensity is enhanced in one directional field distribution as expected when backed with multiple layers of metamaterials, which is not the case for MI communication using only circular loop antennas. In this paper, it has been proved that the presence of metal in the vicinity of the MMLPA system can increase the received power as well. Therefore, this novel communication system can be applied for IoT devices working on the 2.4 GHz and 315 MHz band. Since the antennas are low profile, they can be mounted to buildings' wall and it will become a smart wall, or under cars for smart transportation, etc. Consequently, they are suitable for connecting IoT devices in complex environments especially in near metal environments. Further improvements to the technique should allow a full study of the effect of the communication media especially when operating at lower frequency band.

References

[1] H. Guo, Z. Sun: M2I: Channel modeling for metamaterial enchanced magnetic induction communications, in *Ant. and prop., IEEE trans.*, 2015, 5072–5087.

[2] X. Chen, T. M Grzegorczyk, B. Wu, J. Pacheco, A. Kong: Robust Method to retrieve the constitutive effective parameters of metamaterials, in *Physics Review*, 2004.

[3] D. M. Elsheakh and E. A. Abdallah: Different Feeding Techniques of Microstrip Patch Antennas with Spiral Defected Ground Structure for Size Reduction and Ultra-Wide Band Operation, *Journal of Electromagnetic Analysis and Applications*, 4:1 (2012), 410–418.

[4] Garcia, C. Roman: 3D printed spatially variant anisotropic metamaterials, in *ETD Collection for University of Texas*, El Paso. AAI10118141.

[5] Frequency bands of operation for the Internet of Things: *https://iot-daily.com/2015/03/18/frequency-bands-optimal-for-the-internet-of-things/*, Accessed in July 2018.

[6] A. Balanis: *Antenna theory: analysis and design*, John Wiley & Sons, Hoboken, New Jersey, 2016.